ADVANCES IN ATMOSPHERIC SCIENCES, VOL. 26, NO. 4, 2009, 656–665

Harmonious Inter-decadal Changes of July–August Upper Tropospheric Temperature Across the North Atlantic, Eurasian Continent, and North Pacific

ZHOU Tianjun*[1] (周天军) and ZHANG Jie[1,2] (张 洁)

[1] *State Key Laboratory of Numerical Modeling for Atmospheric Sciences and Geophysical Fluid Dynamics, Institute of Atmospheric Physics, Chinese Academy of Sciences, Beijing* 100029

[2] *Graduate University of Chinese Academy of Sciences, Beijing* 100049

(Received 16 January 2009; revised 21 March 2009)

ABSTRACT

The authors have developed an integral view of the inter-decadal variability of July–August (JA) tropospheric temperature across the entire subtropical Northern Hemisphere. Using reanalysis data and complementary balloon-borne measurements, the authors identify one major mode of variability for the period 1958–2001 which exhibits a significant cooling center over East Asia and warming centers over the North Atlantic and North Pacific. The cooling (warming) signals barotropically penetrate through the troposphere, with the strongest anomalies at 200–300 hPa. The amplitude of the cooling over East Asia is stronger than that of the warming over the North Atlantic (North Pacific) by a factor of 2 (3). This dominant mode exhibits a declining tendency for the entire period examined, particularly before 1980. After the mid-1980s, the tendency has leveled off. Variations of the harmonious change of JA upper tropospheric temperature represented by the principal component of Empirical Orthogonal Function analysis exhibit significant negative (positive) correlations with SST anomalies in the eastern tropical Pacific and the western tropical Indian Ocean (mid-latitude North Pacific). Possible mechanisms are discussed.

Key words: tropospheric temperature, inter-decadal variability, harmonious changes

Citation: Zhou, T. J., and J. Zhang, 2009: Harmonious inter-decadal changes of July–August upper tropospheric temperature across the North Atlantic, Eurasian continent, and North Pacific. *Adv. Atmos. Sci.*, **26**(4), 656–665, doi: 10.1007/s00376-009-9020-8.

1. Introduction

Temperature changes are one of the most obvious and easily measured changes in climate. Previous discussions of climate change have tended to focus on past and future changes in surface air temperature (e.g., Wang and Gong, 2000; Jones and Moberg, 2003; Zhou and Yu, 2006). Since most climate change processes occur in the troposphere, any assessment of climate change and variability should consider both the surface and the troposphere. Great efforts have been devoted to the investigation of tropospheric temperature change in recent years, and new analyses of balloon-borne and satellite measurements of lower- and mid-tropospheric temperature show warming rates that are similar to those of the surface temperature record (Trenberth et al., 2007).

The tropospheric temperature variation exhibits regional features. For example, contrary to the warming trend elsewhere, a spring cooling trend extending from surface to tropopause is found across the subtropical Eurasia continent over the last half century (Yu and Zhou, 2004). Variations of tropospheric temperature over East Asia show distinctive features, partly due to the complex topography. A recent examination of the spring tropospheric temperature change over the eastern flank of the Tibetan Plateau revealed the contribution of the plateau to a cooling shift via continental stratiform cloud-climate feedback (Yu et al., 2004a; Li et al., 2005). The significance of the Ti-

*Corresponding author: ZHOU Tianjun, zhoutj@lasg.iap.ac.cn

betan Plateau as an elevated heat source for the abrupt seasonal change and Asian monsoon onset has been discussed by many authors (e.g., Ye and Gao, 1979). Seasonal upper tropospheric warming over the eastern Tibetan Plateau has been suggested to be the primary cause of the reversals of the meridional temperature gradient associated with monsoon onset. Variations of tropospheric temperature over the plateau contribute to the South (East) Asian summer monsoon, via changes of the meridional (zonal) land-sea thermal contrast (Li and Yanai, 1996; Wu, 2005; Zhao et al., 2007).

East Asian climate has experienced an inter-decadal scale transition near the end of 1970s (Hu, 1997; Wang, 2001; Hu et al., 2003; Han and Wang, 2007). Associated with the inter-decadal climate transition, a strong tropospheric cooling trend is prominent over East Asia during July and August, which contributes to the tendency toward increased droughts in northern China and floods along the Yangtze River valley (often referred to as South China Flood and North China Drought) through changes to the East Asian atmospheric circulation (Yu et al., 2004b). This cooling trend has been verified recently by balloon-borne measurements (Duan, 2007; Yu and Zhou, 2007). A similar mechanism applies to the spring-time inter-decadal scale climate change over south-eastern China, which has been manifested as a tendency toward drought over the past half century (Xin et al., 2006). However, previous discussions only focused on East Asia and have ignored the fact that a warming trend is also evident over the mid-latitude North Atlantic and North Pacific accompanying the cooling over East Asia (c.f. Fig. 1 of Yu et al., 2004b). The present study aims to address the following questions: (1) Is the tropospheric temperature change over East Asia significantly related to temperature changes over the North Atlantic and North Pacific? (2) What is the dominant mode of the tropospheric temperature change across the North Atlantic, Eurasian continent, and North Pacific? Based on reanalysis data and complementary balloon-borne measurements, we show that the tropospheric temperature cooling over East Asia is a local manifestation of a major mode of variability for the period 1958–2001, which exhibits a significant cooling center over East Asia and warming centers over the North Atlantic and North Pacific. This dominant mode exhibits a declining tendency for the entire period examined. After the mid-1980s, however, this tendency has leveled off.

The rest of the paper is organized as follows. We first introduce the data and analysis methods in section 2. We then present the results in section 3. A discussion is given in section 4. Section 5 summarizes the main findings.

2. Data and methods description

The data used in the present study consist of: (1) the European Centre for Medium-Range Weather Forecasts 40-Year Reanalysis (ERA-40) dataset from 1958 to 2001 (Uppala et al., 2005); (2) the Hadley Centre's radiosonde temperature product HadAT, which contains globally gridded radiosonde temperature anomalies from 1958 to present (Thorne et al., 2005); (3) the National Centers for Environmental Prediction/National Center for Atmospheric Research (NCEP/NCAR) reanalysis data from 1958 to 2001 (Kalnay et al., 1996); and (4) observational SST data obtained from the Global Sea-Ice and Sea Surface Temperature (GISST) dataset (Rayner et al., 2003).

In addition to observational data, two sets of model output are used. The first is the global SST-forced ensemble simulation of National Center for Atmospheric Research CAM2.0.1 model (hereafter CAM2) (http://www.ccsm.ucar.edu/models/ccsm2.0.1/cam/camUsersGuide/). Fifteen runs were carried out using CAM2 and observed SST from January 1949 to October 2001 (http://www.ccsm.ucar.edu/working_groups/Variability/index.html). Output of the ensemble simulation has already been used in many studies, e.g., the forcing of El Niño upon the Southern Annular Mode (Zhou and Yu, 2004), the remote forcing of sea surface temperature near the maritime continent and equatorial central-eastern Pacific on the inter-annual and inter-decadal variability of the summer-time western Pacific subtropical high (Wu and Zhou, 2008), the dominance of the warming trend over the central-eastern Pacific and the western tropical Indian Ocean on the decreasing tendency of global land monsoon precipitation in the past half century (Zhou et al., 2008a), and the predictability of Asian-Australian monsoon circulations (Zhou et al., 2008b). The second model output data source is the 20th century climate simulation of CCSM3 (Collins et al., 2006), which has been conducted for the IPCC AR4 under the leadership of the Joint Scientific Committee/Climate Variability and Predictability of the World Climate Research Programme (WCRP) Working Group on Coupled Modeling (WGCM). The simulation was made with various combinations of forcing agents including greenhouse gases (GHGs), sulfate aerosols, as well as volcanic aerosols and solar variability. Time-varying tropospheric and stratospheric ozone forcing has also been included during the model simulation. The CCSM3 model has reasonable performance in reproducing the 20th century surface air temperature evolution, based on an evaluation by Zhou and Yu

(2006).

The statistical methods used in this study include correlation analysis, regression analysis, power spectra analysis, and Empirical Orthogonal Function (EOF) analysis method. The student's t-test, F-test, and Mann-Kendall rank statistics (Sneyers, 1990) were used to test the significance of linear trends.

3. Results

3.1 *The leading mode of tropospheric temperature variability in reanalysis*

Previous studies have found that the "South China flood and North China drought" rainfall pattern associated with the inter-decadal scale climate transition occurred by the end of 1970s is most significant in July and August (JA), and the inter-decadal scale tropospheric cooling over East Asia is also significant in JA (Yu et al., 2004b; Yu and Zhou, 2007). Hence, the analyses presented below mainly focus on the JA mean conditions. We begin our study on the harmonious changes of July–August upper tropospheric temperature across the North Atlantic, Eurasian continent, and North Pacific by analyzing the long-term trends. The linear trends are estimated as the slope of a straight line fitted (in a least squares sense) to the observed anomalous troposphere temperature data at each grid point, based on the reference periods defined. Figure 1a shows the linear trends in the JA mean upper troposphere temperature (250–300 hPa slab-averaged) across the entire 44 years. The prominent features include a significant cooling center located over East Asia and two warming centers located over the North Atlantic and the North Pacific. The amplitude of the cooling center over East Asia is 0.5 K $(10\ \mathrm{yr})^{-1}$. The amplitude of the warming center over the North Atlantic (North Pacific) is 0.4 K $(10\ \mathrm{yr})^{-1}$ [0.3 K $(10\ \mathrm{yr})^{-1}$]. The cooling is far stronger than the warming in strength. The center over East Asia resembles that shown in Yu et al. (2004b). It should be noted that the cooling and warming anomalies are significant from 500 hPa to 200 hPa, reaching a maximum at 250–300 hPa. To highlight the anomalies, we confine the core analyzed levels to 250–300 hPa in this study.

Since the linear trend does not definitively indicate inter-decadal scale variations, we further explore the coherent variation of tropospheric temperature change across Northern Hemisphere by performing EOF analysis upon the JA mean temperature anomalies. Figure 1b shows the spatial pattern of the first leading EOF mode of the 250–300 hPa slab-averaged temperature anomalies, which is obtained by analysis of the correlation matrix based on the ERA40 data set. The fractional variance of the first leading EOF mode is 22.2%. The EOF2 mode (pattern not shown) accounts for 13.2% of the total variance. According to the rule of North et al. (1982), the observed first two leading modes are well distinguished from each other in terms of the sampling error bars, and hence are statistically significant. A same analysis based on the NCEP/NCAR reanalysis shows similar features, indicating the dataset-independence of the result of EOF analysis (figure not shown). Given the resemblance of the trends of the EOF1 modes, we focus our discussion on the first leading mode here. The first leading mode reflects a zonal land-sea asymmetry pattern, which is dominated by three anomalous centers located over the North Atlantic, East Asia, and the North Pacific, respectively. This distribution closely resembles Fig. 1a except with a reversed sign, having a pattern correlation coefficient of -0.75. The pattern correlation coefficient is calculated as temporal correlation but uses data at all gridpoints instead of time samples. The corresponding principal component (hereafter PC1) is given in Fig. 1c, which shows a decreasing tendency for the entire period examined, particularly before 1980. The linear trend of the PC is $-2.5\ (50\ \mathrm{yr})^{-1}$, which is significantly different from zero at the 1% confidence level based on Mann-Kendall rank statistics. Note that before performing EOF analysis, the zonal mean condition has been subtracted from the raw data. If we directly perform EOF analysis on the raw data, the EOF1 mode presented above appears as the EOF2 mode, and the explained variance is nearly the same (figures not shown).

The leading mode of Northern Hemisphere tropospheric temperature change is featured by the three anomalous centers located over the North Atlantic, East Asia, and the North Pacific, respectively. To exhibit evolutions of the upper tropospheric temperature over the above three target domains, the time series of JA 250–300 hPa mean anomalous temperature averaged respectively over three core areas (i.e., the central shaded areas over the North Atlantic, East Asia, and North Pacific shown in Fig. 1b) are presented in Fig. 2. Both the North Atlantic and the North Pacific show warming trends in the upper troposphere, particularly before the late 1980s. The warming trend over the North Pacific is more significant before the late 1970s. In fact, after the late 1980s, there appears to be a slightly decreasing tendency. The warming trend over the North Atlantic has also leveled off since the mid-1980s. In contrary to the conditions of the North Atlantic and North Pacific, the upper troposphere over East Asia exhibits a robust cooling trend, particularly before the 1980s, as evidenced in Yu et al. (2004b).

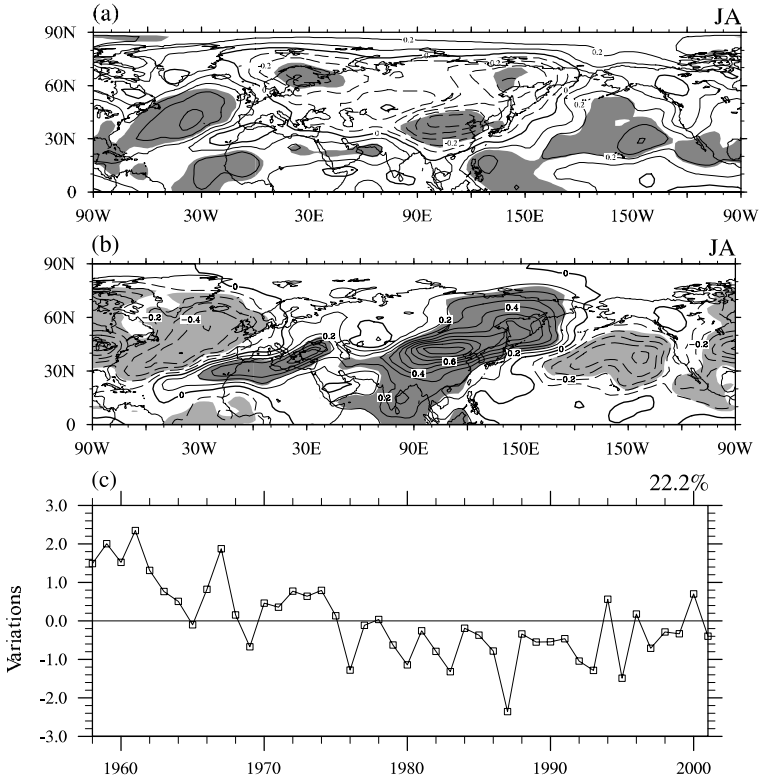

Fig. 1. (a) Trends of JA slab-averaged temperature anomalies between 250 hPa and 300 hPa, units: K (10 yr)$^{-1}$. Areas exceeding a confidence level of 95% using an F-test are shaded. (b) Spatial pattern of the leading Empirical Orthogonal Function (EOF) mode of the JA 250–300 hPa slab-averaged temperature and (c) the corresponding principle component (unitless). The air temperature data come from the ERA-40 and the zonal mean condition has been subtracted before performing EOF analysis. The EOF pattern of (b) is shown as the temperature anomalies regressed upon the associated PC (unitless). The shadings outline the regions exceeding a confidence level of 99% using student's t-test.

The variation is relatively stable after the 1980s and has no significant trend. Hence, there appears to be a harmonious change of the upper tropospheric temperature across the mid-latitudes (30°–60°N) for the North Atlantic, the Eurasian continent, and the North Pacific. This harmony is further demonstrated by the significant correlations among the indices, as shown in Table 1. While the North Atlantic and the North Pacific are positively correlated with each other in the defined indices, having a correlation coefficient of 0.59, which is statistically significant at the 5% level, both of them have significant negative correlations (i.e., −0.80 and −0.77, both statistically significant at the 0.05 level) with East Asia in the upper tropospheric temperature variations. After removing the linear trends, the corresponding correlation coefficients decrease slightly, but are still nearly significant at the 0.05 level by using student's t-test.

3.2 *The tropospheric temperature variation in radiosonde data*

The analyses outlined above are based on the 250–300 hPa data in reanalysis. Visual inspections of Figs. 1–2 show that there are some transition or jump points. For example, a conspicuous jump is evident in 1968/69 in Figs. 1c and 2a, and weaker jumps are also visible in Figs. 2b–c. Since the 250 hPa level became a standard pressure level in the late 1960s and most radiosonde stations did not report at this level before 1968, it is possible that the introduction of these data has introduced a spurious jump-like signal in the reanalysis, which depends only on radiosonde data at high levels. To confirm that the results found here are not based on spurious signals in the reanalysis, and also to reduce uncertainties relevant to the quality of reanalysis data, the time series of 250–300 hPa mean temperature averaged over the three target domains is

Table 1. Correlation coefficients among three tropospheric temperature indices derived from ERA-40 reanalysis shown in Fig. 2 (solid lines). The correlation coefficients between the indices after removing the linear trends are listed in parentheses.

	North Atlantic	East Asia	North Pacific
North Atlantic	1.0 (1.0)	−0.80 (−0.61)	0.59 (0.29)
East Asia	−0.80 (−0.61)	1.0 (1.0)	−0.77 (−0.56)
North Pacific	0.59 (0.29)	−0.77 (−0.56)	1.0 (1.0)

also calculated by employing the HadAT data set, which is a quality-controlled, widely used radiosonde dataset (Thorne et al., 2005). The good quality of the HadAT dataset over East Asia has recently been assessed and demonstrated by Li et al. (2008a). As shown in Fig. 2, the index derived from the HadAT data strictly matches that derived from the ERA-40 data, having a correlation coefficient of 0.92 (0.86) for the North Atlantic (East Asia). Since only a limited number of data are available over the North Pacific in the HadAT data set, the correlation between the time series derived from two data sets is 0.52, which is slightly lower than over the North Atlantic and East Asia, but still statistically significant at the 0.05 level. Further analyses based on the NCEP/NCAR reanalysis data (Kalnay et al., 1996) also revealed highly consistent results (figures not shown), adding fidelity to the robustness of the results.

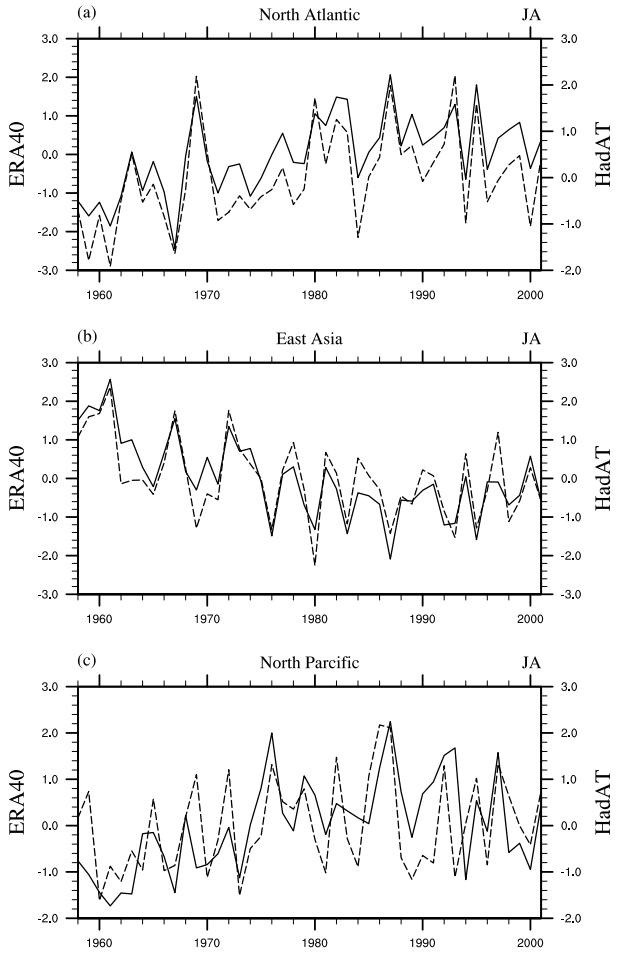

Fig. 2. Normalized time series of JA 250–300 hPa mean temperature averaged over (a) the North Atlantic, (b) East Asia (East Asian tropospheric temperature index), and (c) the North Pacific. The result derived from ERA-40 (HadAT) is shown in solid (dashed) lines and corresponds to the left (right) ordinate. The zonal mean value has been subtracted before analysis. The three regional averages are calculated respectively within their core regions, and statistically significant areas are shown in Fig. 1b (unitless).

We have also calculated lead-lag correlations between the East Asian and North Atlantic index time series, and between the East Asian and North Pacific index time series, and the largest correlations occur at zero-lag (figures not shown), implying no cause-and-effect relationship among the upper tropospheric temperature variations across the North Atlantic, Eurasia continent, and the North Pacific.

3.3 *The vertical structure of tropospheric temperature change*

The harmonious change of troposphere temperature outlined above is further verified by calculating the correlation coefficients between the temperature anomalies at each gridpoint and the index of East Asia shown in Fig. 2b. The result is presented in Fig. 3a. It is not surprising to see three zonally distributed "negative-positive-negative" centers which closely resemble the patterns of Figs. 1a–b.

To have a much clearer picture of the vertical structure of the temperature anomalies, a longitude-height cross-section of the correlation coefficient averaged between 30°N and 45°N is presented in Fig. 3b. A zonally tri-polar pattern stands out in the panel, with one positive center over the East Asia, and two negative centers over the North Atlantic and North Pacific, respectively. The signals penetrate throughout the troposphere, indicating a barotropic structure. The largest anomalies appear near the 200–300 hPa levels in the vertical. Hence, the harmonious change of the temperature across the North Atlantic, Eurasian con-

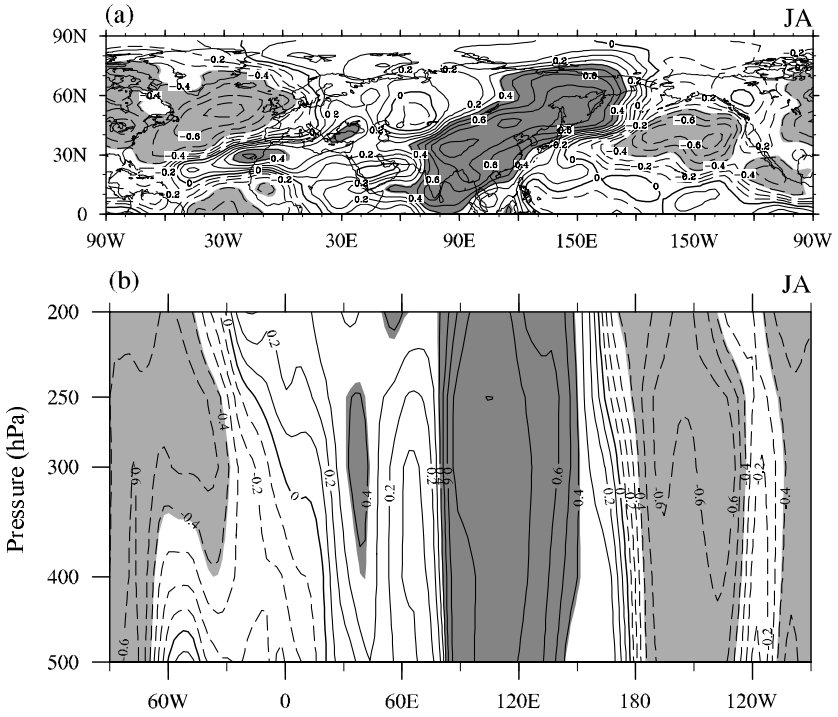

Fig. 3. (a) Spatial pattern and (b) longitude-height cross-section of the correlation coefficient between the JA 250–300 hPa slab-averaged temperature anomalies and the East Asian tropospheric temperature index (units: K). The shadings outline the regions exceeding a confidence level of 99% using student's t-test. Panel (b) is for the meridional average between 30°–45°N. The zonal mean value has been subtracted before analysis.

tinent, and North Pacific is not limited to the upper troposphere; rather, it extends vertically throughout most parts of the troposphere.

The vertical barotropic structure of temperature change also adds fidelity to the results presented here. The vertical homogeneous variation of temperature from 200 hPa to 500 hPa demonstrates that the signal is reliable, since the 250 hPa has become a standard pressure level only since the late 1960s, and the 200-hPa, 300-hPa, and 500-hPa levels have been standard pressure levels for a much longer time, as discussed in the section above. The vertical homogeneous signal suggests that if we use 200–300-hPa average temperature rather than 250–300-hPa average temperature to perform EOF analysis, we would get a similar pattern as Fig. 1b. This speculation has been confirmed by our analysis (figures not shown).

3.4 *The time scales of harmonic tropospheric temperature change*

The significant correlations among the temperature changes across the North Atlantic, Eurasian continent, and North Pacific are not purely due to the long-term trend, as evidenced in Fig. 2. To quantitatively reveal the dominant time scales of the coherent variability, we have calculated the power spectra of the three indices shown in Fig. 2 and the PC1 shown in Fig. 1c. The result is presented in Fig. 4. All indices have a common spectral peak around 3 years, signaling coherent interannual variations in the low frequency (LF) band. A secondary spectral peak at 2.1 years signaling the quasi-biennial (QB) variability is also evident in the PC1, North Atlantic, and North Pacific indices, and slightly weaker in the East Asian index.

It is interesting to note that a recent analysis of global land monsoon precipitation found the North African, South American, and Australian monsoons having stronger spectral power in the LF band, while the South African and South and East Asian monsoons have greater power in the QB band (Zhou et al., 2008c). Many previous studies have been devoted to the connections of upper troposphere cooling change with the surface climate (precipitation and surface air temperature) at inter-decadal time scales (e.g., Yu et al., 2004b; Li et al., 2005; Xin et al., 2006; Yu and Zhou, 2007), while less attention has been paid to the connection at inter-annual time scales. The resemblance of the spectral peaks presented here suggests that the potential connection of troposphere temperature change with monsoon climate at inter-annual time

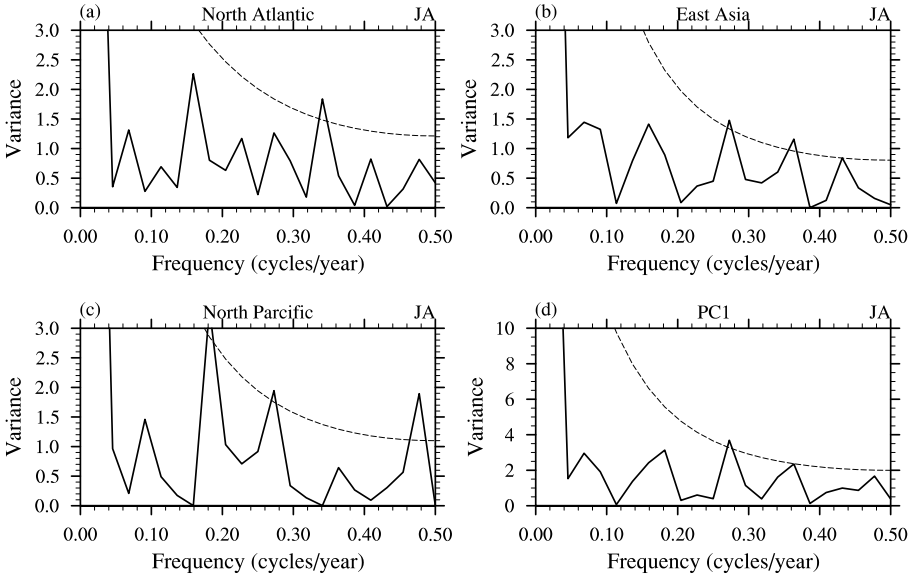

Fig. 4. Power spectra of (a) the North Atlantic, (b) East Asia, and (c) the North Pacific tropospheric temperature index shown in Fig. 2. (d) Power spectra of PC1 shown in Fig. 1c. The thin dashed line is the red noise power density. A spectrum with a peak above the thin dashed line implies it distinguishes from a red noise spectrum with a confidence level over 90%. The unit of abscissa is yr^{-1}.

scales deserves further study.

4. Discussion

The analyses outlined above have developed an integral view of the inter-decadal and inter-annual variabilities of July–August mean tropospheric temperature across the entire subtropical Northern Hemisphere. While the picture of the harmonious changes is clear, the mechanisms responsible for the temperature changes are unknown. Since the detailed evolution of weather events may not be predictable beyond a few days to two weeks due to the chaotic internal dynamics of the atmospheric motion, the long-term harmonious change of the upper troposphere across the North Atlantic, Eurasian continent, and North Pacific might be due to the interactions between the atmosphere and the more slowly varying oceans and land surface processes. To reveal the potential contribution of the slowly varying oceans, the JA SST anomalies are correlated with PC1 (i.e., Fig. 1c). As shown in Fig. 5a, significant negative (positive) correlations are observed over the eastern tropical Pacific and the western tropical Indian Ocean (mid-latitude North Pacific). The pattern of SST anomalies closely resembles that responsible for the decreasing tendency of global land monsoon precipitation in the past half century (Zhou et al., 2008a).

Given the significant correlations with the SST, it is desirable to examine whether the tropospheric temperature changes that have been detected follow from the atmosphere's response to the observed SST variations. To gain insight into this question, we employ an Atmospheric Model Intercomparison Project (AMIP)-model approach. The SST-induced changes in the upper tropospheric temperature over the past 44 years (1958–2002) are examined by using a set of atmospheric general circulation model (AGCM) (i.e., CAM2) ensembles forced by observed monthly historical SST data. To reduce the impact of internal noise, only the result of ensemble mean is analyzed. The regression coefficients of the simulated 250–300-hPa mean temperature anomalies upon the observed PC1 are shown in Fig. 5b. Unfortunately, no close resemblance can be found between the simulation and the observations (cf., Fig. 5b and Fig. 1b). For example, the air over the East Asian continent is dominated by significant positive correlations in Fig. 1b, but by significant negative correlations in Fig. 5b. Only over northeastern Asia near 50°N, 150°E does the simulation partly resemble the observation with a significant positive correlation. There is no similarity over the North Atlantic and North Pacific between the observations and the simulation. This discrepancy suggests that the SST anomalies shown in Fig. 5a may not be a forcing mechanism for the detected tropospheric temperature changes, although the weak extra-tropical atmospheric responses of AGCM results to specified SST forcing may be another reason. This is, in some extent, coincident with Zhao et al. (2008), who noted

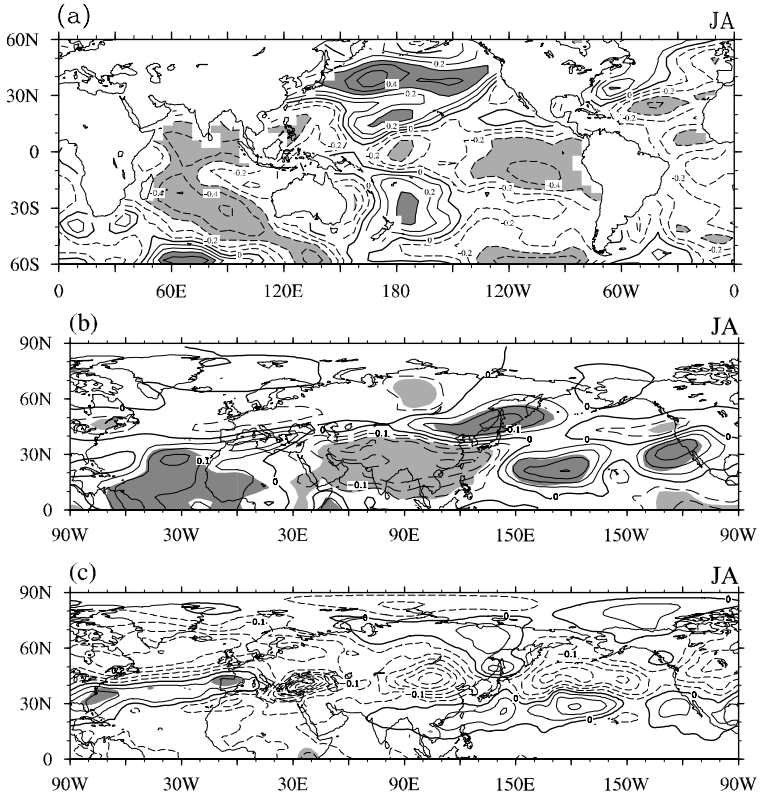

Fig. 5. (a) Distribution of correlation coefficient between JA SST anomalies and the PC1 of Fig. 1c. Spatial pattern of the (b) CAM2 and (c) CCSM3 model simulated JA 250–300 hPa slab-averaged temperature anomalies regressed upon the observed PC1 shown in Fig. 1c (unitless). The shadings outline the regions exceeding a confidence level of 95% using student's t-test.

that the SST anomalies in the Pacific could not induce the observed temperature anomalies in the upper troposphere. Determining whether the response is model-dependent or not also requires further investigation. There is evidence suggesting that the cooling of the upper troposphere over East Asia may be partly reproduced by using the most recent version of the NCAR CAM3 model (Li et al., 2008b).

Climate change in the upper atmosphere may be related to the change of ozone amount. Ozone depletion would result in less solar radiation absorbed in the upper troposphere. Recent analysis revealed a declining trend of the ozone amount over the Tibetan Plateau (hereafter TP) (Zou, 1996), which has been used to explain the observed cooling trend in the upper troposphere over the TP (Duan, 2007). To verify this potential mechanism, the output of the 20th century climate simulation of the CCSM3 model is used. The historical changes of ozone have been specified during the simulation. The simulated 250–300-hPa mean temperature anomalies are regressed upon the observed PC1. The result is presented in Fig. 5c. The model also failed in producing the observed tropospheric temperature anomalies (cf., Fig. 5c and Fig. 1c). The simulated troposphere over East Asia is dominated by insignificant negative anomalies, not like the observations which are dominated by significant positive anomalies. This discrepancy suggests the ozone depletion may not be a contributor. However, it also should be noted that stratospheric-tropospheric interaction is not represented perfectly even in current state-of-the-art climate models such as CCSM3, and so the impacts of ozone on tropospheric climate may not be correctly simulated. There is a possibility that the unreasonable response of tropospheric temperature may be due to the model performance. Future examinations employing middle atmosphere AGCMs such as the SOCOL model (Egorova et al., 2003) may help us in understanding this issue. The mechanism responsible for the harmonious change of upper tropospheric temperature remains an open question. Additional study is needed to understand the physical processes behind the detected signals.

A previous study has argued that the inter-decadal

change of the upper tropospheric temperature over East Asia in June is different from that in July–August, with a moderate warming rather than cooling being observed in recent decades (Yu and Zhou, 2007). We have examined the changes of June upper tropospheric temperature over the Northern Hemisphere, and could not find similar harmonic changes as that of JA (figure not shown). This supports the notion in Yu and Zhou (2007) that analysis of the inter-decadal scale climate variability over East Asia should not treat June–July–August as a whole.

In addition, a recent work conducted by Zhao et al. (2007) focused on cooling (warming) temperature anomalies over Asia (Pacific) and defined the Asian-Pacific oscillation (APO) as the difference between vertically averaged (500–200-hPa) eddy temperatures between Asia and the North Pacific. Zhou et al. (2008) found a positive correlation between the APO and the tropical cyclone frequency over the western North Pacific. As a harmonious change of upper tropospheric temperature across the Northern Hemisphere, an integral view of the three oscillation centers is necessary and the climate impact of this harmonious change needs to be addressed. Recent analysis on the global land monsoon precipitation change revealed an overall downward trend; this declining trend has also leveled off since the 1980s (Wang and Ding, 2006), which nearly strictly matches the evolution of the upper troposphere temperature shown in Fig. 1c (c.f., Figs. 2–3 of Wang and Ding, 2006). Whether this kind of coherent variation is connected to the processes governing the temperature changes warrants further study.

5. Summary

We reveal a harmonious change of JA upper tropospheric temperature across the North Atlantic, Eurasian continent, and North Pacific over the last 44 years (1958–2001). It appears as a significant cooling trend centralized in East Asia, and with two warming centers located over the North Atlantic and North Pacific, respectively. The cooling (warming) signals barotropically penetrate throughout the troposphere, with the strongest anomalies at 200–300 hPa. The amplitude of the cooling over East Asia is stronger than that the warming over the North Atlantic (North Pacific) by a factor of 2 (3). This harmonious change pattern accounts for 22.2% of the total variance of the Northern hemispheric upper tropospheric temperature change. The cooling (warming) tendency exists for the entire period, particularly before 1980. After the mid-1980s the tendency has leveled off. In addition to the trend, this harmonic variation also has a dominant time scale of 3 years. This harmonious change of JA upper tropospheric temperature is significantly correlated with negative (positive) SST anomalies in the eastern tropical Pacific and the western tropical Indian Ocean (mid-latitude North Pacific).

Acknowledgements. This work was jointly supported by the China Meteorological Administration (GYHY200706010, GYHY200806010), the Major State Basic Research Development Program of China under Grant Nos. 2006CB403603 and 2005CB321703, and the National Natural Science Foundation of China under Grant Nos. 40523001, 40625014, and 90711004.

REFERENCES

Collins, W. D., and Coauthors, 2006: The Community Climate System Model version 3 (CCSM3). *J. Climate*, **19**(11), 2122–2143.

Duan, A., 2007: Cooling trend in the upper troposphere and lower stratosphere over China. *Geophys. Res. Lett.*, **34**, L15708, doi: 10.1029/2007GL029667.

Egorova, T., E. Rozanov, V. A. Zubov, and I. L. Karol, 2003: Model for investigating ozone trends (MEZON). Izvestiya. *Atmospheric and Oceanic Physics*, **39**, 277–292.

Han, J., and H. Wang, 2007: Interdecadal variability of the East Asian summer monsoon in an AGCM. *Adv. Atmos. Sci.*, **24**, 808–818, doi: 10.1007/s00376-007-0808-0.

Hu, Z.-Z., 1997: Interdecadal variability of summer climate over East Asia and its association with 500 hPa height and global sea surface temperature. *J. Geophys. Res.*, **102**(D16), 19403–19412.

Hu, Z.-Z., S. Yang, and R. Wu, 2003: Long-term climate variations in China and global warming signals. *J. Geophys. Res.*, **108**(D19), 4614, doi: 10.1029/2003JD003651.

Jones, P. D., and A. Moberg, 2003: Hemispheric and large-scale surface air temperature variations: An extensive revision and an update to 2001. *J. Climate*, **16**(2), 206–223.

Kalnay, E., and Coauthors, 1996: The NCEP/NCAR 40-Year Reanalysis Project. *Bull. Amer. Meteor. Soc.*, **77**(3), 437–471.

Li, C. F., and M. Yanai, 1996: The onset and interannual variability of the Asian summer monsoon in relation to land-sea thermal contrast. *J. Climate*, **9**(2), 358–375.

Li, J., R. Yu, T. Zhou, and B. Wang, 2005: Why is there an early spring cooling shift downstream of the Tibetan Plateau. *J. Climate*, **18**(22), 4660–4668.

Li, J., R. Yu and T. Zhou, 2008a: Teleconnection between NAO and climate downstream of the Tibetan Plateau. *J. Climate*, **21**, 4680–4690.

Li, H., A. Dai, T. Zhou, and J. Lu, 2008b: Responses of East Asian summer monsoon to historical SST and atmospheric forcing during 1950–2000. *Climate Dyn.*, doi: 10.1007/s00382-008-0482-7.

North, G. R., T. L. Bell, R. F. Cahalan, and F. J. Moeng,

1982: Sampling errors in the estimation of Empirical Orthogonal Functions. *Mon. Wea. Rev.*, **110**, 699–706.

Rayner, N. A., D. E. Parker, E. B. Horton, C. K. Folland, L. V. Alexander, D. P. Rowell, E. C. Kent, and A. Kaplan, 2003: Global analyses of sea surface temperature, sea ice, and night marine air temperature since the late nineteenth century. *J. Geophys. Res.*, **108**(D14), 4407, doi: 10.1029/2002JD002670.

Sneyers, R., 1990: On the statistical analysis of series of observations. WMO Technical Note 143, WMO No. 415, TP-103, Geneva, World Meteorological Organization, 192pp.

Thorne, P. W., D. E. Parker, S. F. B. Tett, P. D. Jones, M. McCarthy, H. Coleman, and P. Brohan, 2005: Revisiting radiosonde upper air temperatures from 1958 to 2002. *J. Geophys. Res.*, **110**, D1805, doi: 10.1029/2004JD005753.

Trenberth, K. E., and Coauthors, 2007: Observations: Surface and atmospheric climate change. *Climate Change 2007: The Physical Science Basis*. Solomon et al., Eds., Cambridge University Press, Cambridge, United Kingdom and New York, NY, USA, 235–335.

Uppala, S. M., and Coauthors, 2005: The ERA-40 reanalysis. *Quart. J. Roy. Meteor. Soc.*, **131**(612), 2961–3012.

Wang, B., and Q. H. Ding, 2006: Changes in global monsoon precipitation over the past 56 years. *Geophys. Res. Lett.*, **33**, L06711, doi: 10.1029/2005GL025347.

Wang, H., 2001: The weakening of Asian monsoon circulation after the end of 1970s. *Adv. Atmos. Sci.*, **18**, 376–386.

Wang, S. W., and D. Y. Gong, 2000: Enhancement of the warming trend in China. *Geophys. Res. Lett.*, **27**(16), 2581–2584.

Wu, B. Y., 2005: Weakening of Indian summer monsoon in recent decades. *Adv. Atmos. Sci.*, **22**(1), 21–29.

Wu, B., and T. Zhou, 2008: Oceanic origin of the interannual and interdecadal variability of the summertime western Pacific subtropical high. *Geophys. Res. Lett.*, **35**, L13701, doi: 10.1029/2008GL034584.

Xin, X. G., R. C. Yu, T. J. Zhou, and B. Wang, 2006: Drought in late spring of South China in recent decades. *J. Climate*, **19**(13), 3197–3206.

Ye, T., and Y. Gao, 1979: *The Meteorology of the Tibetan Plateau*. Science Press, Beijing, 278pp. (in Chinese)

Yu, R. C., and T. J. Zhou, 2004: Impacts of winter-NAO on March cooling trends over subtropical Eurasia continent in the recent half century. *Geophys. Res. Lett.*, **31**, L12204, doi: 10.1029/2004GL019814.

Yu, R., and T. Zhou, 2007: Seasonality and three-dimensional structure of the interdecadal change in East Asian monsoon. *J. Climate*, **20**, 5344–5355.

Yu, R. C., B. Wang, and T. J. Zhou, 2004a: Climate effects of the deep continental stratus clouds generated by the Tibetan Plateau. *J. Climate*, **17**(13), 2702–2713.

Yu, R. C., B. Wang, and T. J. Zhou, 2004b: Tropospheric cooling and summer monsoon weakening trend over East Asia. *Geophys. Res. Lett.*, **31**, L22212, doi: 10.1029/2004GL021270.

Zhao, P., Y. Zhu, and R. Zhang, 2007: An Asian-Pacific teleconnections in summer tropospheric temperature and associated Asian climate variability. *Climate Dyn.*, **29**, 293–303, doi: 10.1007/s00382-007-0236-y.

Zhao, P., J. M. Chen, D. Xiao, S. L. Nan, Y. Zou, and B. T. Zhou, 2008: Summer Asian Pacific oscillation and its relationship with atmospheric circulation and monsoon rainfall. *Acta Meteorologica Sinica*, **66**(5), 716–729. (in Chinese)

Zhou, B. T., X., Cui, and P. Zhao, 2008: Relationship between the Asian-Pacific Oscillation and the tropical cyclone frequency in the western North Pacific. *Science in China(D)*, **51**(3), 380–385.

Zhou, T. J., and R. C. Yu, 2004: Sea-surface temperature induced variability of the Southern Annular Mode in an atmospheric general circulation model. *Geophys. Res. Lett.*, **31**, L24206, doi: 10. 1029/2004GL021473.

Zhou, T. J., and R. C. Yu, 2006: Twentieth-century surface air temperature over China and the globe simulated by coupled climate models. *J. Climate*, **19**(22), 5843–5858.

Zhou, T., R. Yu, H. Li, and B. Wang, 2008a: Ocean forcing to changes in global monsoon precipitation over the recent half century. *J. Climate*, **21**(15), 3833–3852.

Zhou, T., and Coauthors, 2008b: The CLIVAR C20C Project: Which components of the Asian-Australian Monsoon circulation variations are forced and reproducible? *Climate Dyn.*, doi: 10.1007/s00382-008-0501-8.

Zhou, T., L. Zhang, and H. Li, 2008c: Changes in global land monsoon area and total rainfall accumulation over the last half century. *Geophys. Res. Lett.*, **35**, L16707, doi: 10.1029/2008GL034881.

Zou, H., 1996: Seasonal variation and trends of TOMS ozone over Tibet. *Geophys. Res. Lett.*, **23**(9), 1029–1032.